600.446: Advanced Computer Integrated Surgery

Final Project Report

Robotically Assisted Cochlear Imaging and Access

Ehsan Azimi, Berk Gonenc

Mentors: Russell Taylor, Iulian Iordachita, Jin Kang, John Niparko, Wade Chien

May 10, 2012

Abstract

Cochlear implants are electronic devices that are used to restore hearing to individuals with severe-to-profound sensorineural loss via direct stimulation of the auditory nerve. Implantation requires the insertion of an electrode into human cochlea, which is associated with several challenges and severe complications. In this study, a new approach is developed that incorporates the cooperative control of a steady hand robot along with the intra-operative OCT imaging to generate virtual fixtures that enable the surgeon to insert the implant precisely inside the patient's cochlea without causing trauma.

1. Introduction

Cochlear implant surgery can be an immense auditory, linguistic and developmental benefit to patients with severe hearing deficiencies due to the loss of hair cell transduction within the cochlea. The surgical procedure is potentially complicated by difficulties with implanting electrode array insertion, and serious complications may occur.

One particularly challenging step is the actual insertion of the implant into the cochlea. After accessing the scala tympani (via direct round window insertion, or drilling open a cochleostomry to gain access to the cochlea), an electrode array is inserted into scala tympani of the cochlea. Several designs of cochlear implant arrays have relied on stylet-based insertion techniques. Accordingly, there is a need in the art for a system that allows a surgeon to information regarding the location of the implant with respect to the cochlea walls.

Different groups have reported about force measurement studies for insertion process of the CI electrodes using similar setups with measuring the applied forces outside of the cochlea. However, external force measurements of CI electrode insertions do not reproduce the forces applied to the cochlea by the deformation process of the electrode.

Cochlear implants aim at direct stimulation of the auditory nerve via an electrode array placed inside the cochlea. The state of the art for this operation is a facial recess approach to the middle ear. After the cochleostomy is performed by recess, the array is manually inserted into the scala tympani using special tools such as claws and alligator forceps. Scala tympani is separated from the other two fluid filled compartments inside the cochlea only by a thin basilar membrane as shown in Figure 1. Basilar membrane is a very delicate layer, which accommodates the inner hairy cells that generate the neural activities associated with hearing. Hence any damage on this layer will cause hearing loss or deafness.

Combined electrical and acoustic stimulation (EAS) is a new technique to restore hearing to patients with severe hearing loss, but still with some residual hearing, by amplifying the residual hearing via a hearing aid and simultaneously stimulating the cochlear nerve via an implant. For this strategy, it is very important to preserve the patient's residual hearing during implant surgery. However, using the conventional manual methods, most of this residual hearing is often lost due to various operatively caused traumas [1-10]. The traumas can be attributed to two main sources: cochleostomy, and electrode insertion into scala tympani.
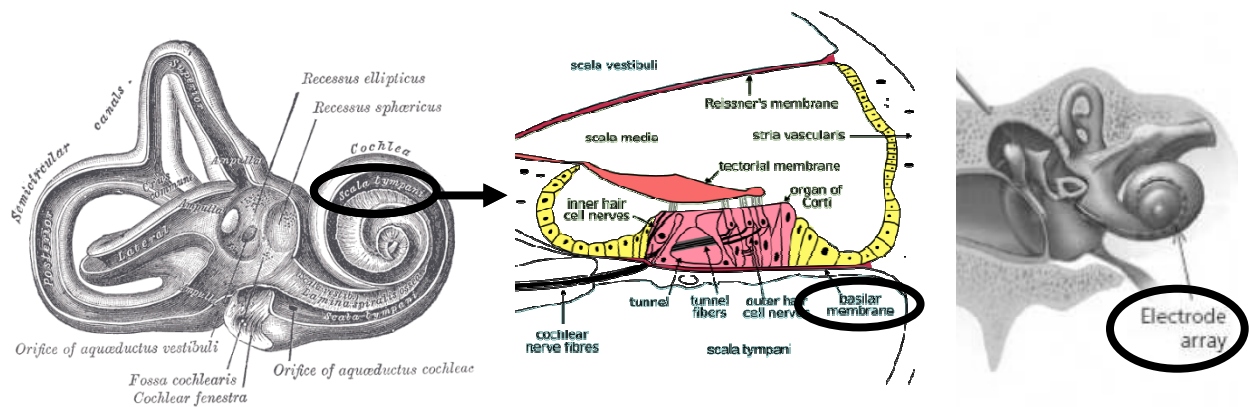
Figure 1 - Scala tympani location and anatomy inner ear. The electrode array is inserted in scala tympani where basilar membrane is located.

As a remedy for the first source, a bone-attached Gough-Stewart parallel robot was proposed to reduce the risk of damaging the facial nerve and the trauma during cochleostomy [18,19]. By using CT scans of the patient, safe optimal trajectories to the cochlea were determined, according to which chorda tympani was drilled.

In order to reduce the insertional trauma, which is the second greatest trauma source, different electrode designs with different insertion behavior were developed recently. More flexible straight implants with lower stiffness were used instead of preformed models. However, patients having a preformed electrode array have shown better results compared to the patients with a straight array [13] since the distance between the active electrodes and cochlear nerve in the central axis of cochlea is minimal for preformed configuration, providing a better perimodiolar position for the electrodes as shown in Figure 2 [11,12].

(a)   (b)
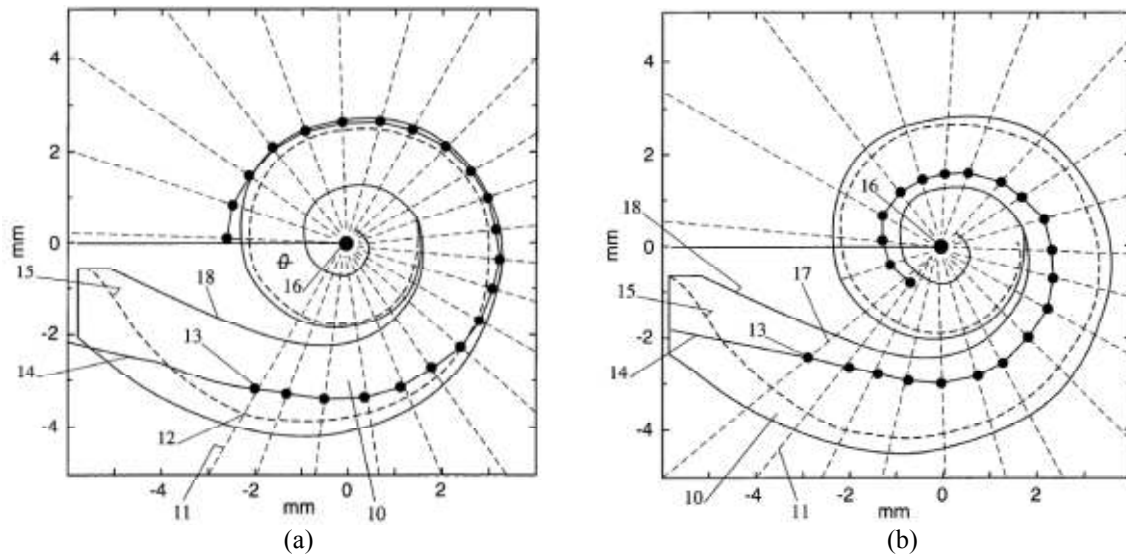
Figure 2 - (a) Position of a straight array far from cochlear nerve (b) Perimodiolar position of preformed array [12].

Currently, an implant that is soft and flexible enough for causing no trauma with perimodiolar placement does not exist. Thus, using a preformed electrode with the right positioning and orientation is still the best alternative. An illustration of this type of electrode from Cochlear Ltd. (Contour Advance electrode) is shown in Figure 3.

Figure 3 - Cochlear Nucleus 24 Contour Advance Practice Electrode. After stylet retraction, the array turns to its preformed state [11].

During the surgery, Advance Off-Stylet(AOS) technique is used to place a preformed electrode inside the cochlea. The insertion is accomplished in 3 steps as shown in Figure 4, which are based on certain landmarks on the electrode array:

a. The array is held straight with a platinum wire stylet. The straight electrode is inserted until the white marker reaches cochleostomy site.

b. Then the platinum stylet is held fixed and silicone electrode carrier is gradually pushed off the stylet inside the cochlear canal. As the stylet is withdrawn, the electrode turns back to its precurled state to follow the inner wall of the cochlea.

**c.** After the ribs reach the cochleostomy site, the stylet is removed.
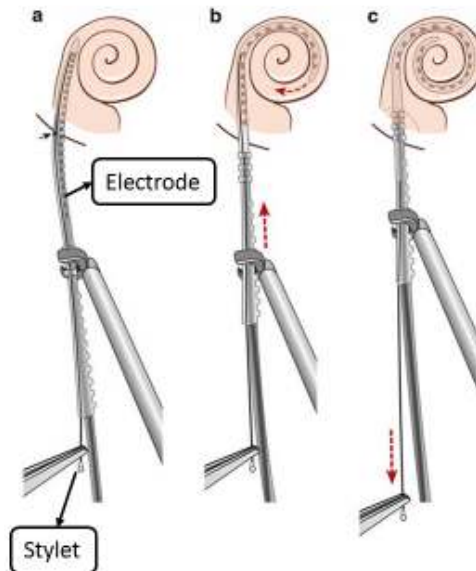
Figure 4 - Advance Off-Stylet technique is performed in 3 steps based on the landmarks on the electrode array [14].

In order to have a model that can describe the geometrical features, curling behavior of these electrodes was analyzed [20]. In this study, an image-processing algorithm was used to detect electrode shape from a series of images. An automatic image-processing procedure was developed to determine the complete curvature of the electrode array by identifying the multiple platinum contacts of the electrode. Consequently, bending characteristics of the electrodes were mathematically modeled by combining a spiral and additional linear functions. The linear terms had to be introduced to represent the initially straightened electrode position as well as the soft tip. Then using a fitting algorithm for nonlinear least-squares problems, a complete mathematical description of the electrode array was provided. The system was tested for curling behavior as a function of stylet extraction. By using such a model, effects like intracochlear wall contact and applied forces could be estimated when realistic anatomical models are integrated into the simulation.

The need for an atraumatic implant insertion and correct placement of the electrode within the scala tympani in AOS has promoted research into a number of automated insertion tools [11, 14-17]. The electrode array was inserted via forceps while a hook was used to retract the stylet. Both of these actions

were performed robotically, which also eliminated hand-tremor problem. In these studies the main focus has been on applied insertion forces. Safe insertion forces were defined based on taken measurements. Suddenly increasing forces indicated touching cochlear walls as a result of either incorrect orientation of the electrode or reaching the basal turn. In this project, we aim to provide similar assistance in AOS by implementing virtual fixtures instead of force sensing. By using OCT imaging techniques, the critical location for drawing the electrode array off stylet can be intra-operatively identified, the virtual fixtures can be accordingly defined. By constraining the motion of the insertion tool via virtual fixtures, any intracochlear trauma can be prevented before touching the walls of the cochlea.
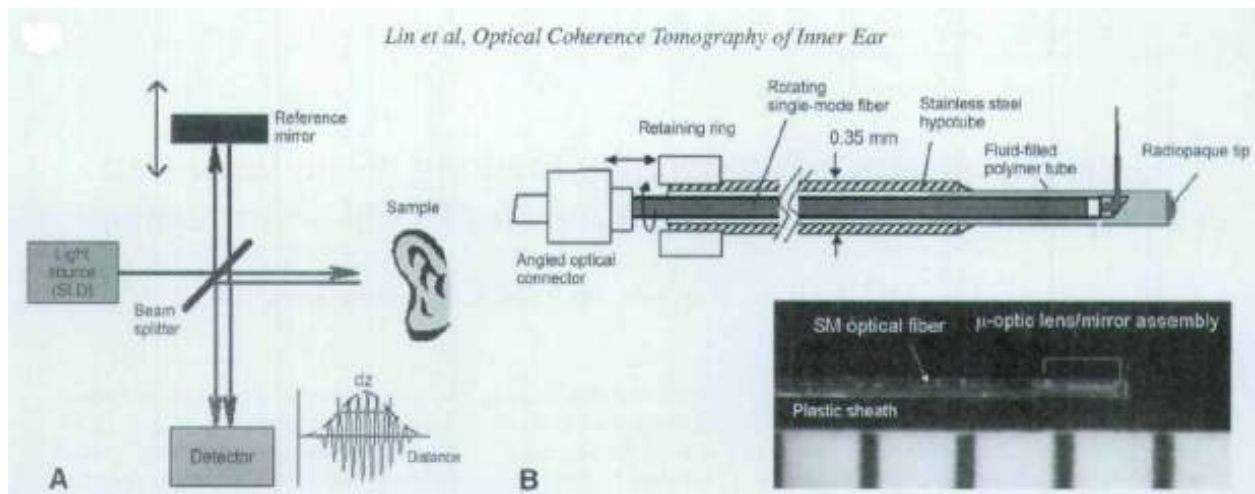
Figure 5 - Schematic of OCT Imaging System [21]. (a) Basic interferometry principle of OCT. (b) Detailed schematic of rotating OCT probe.
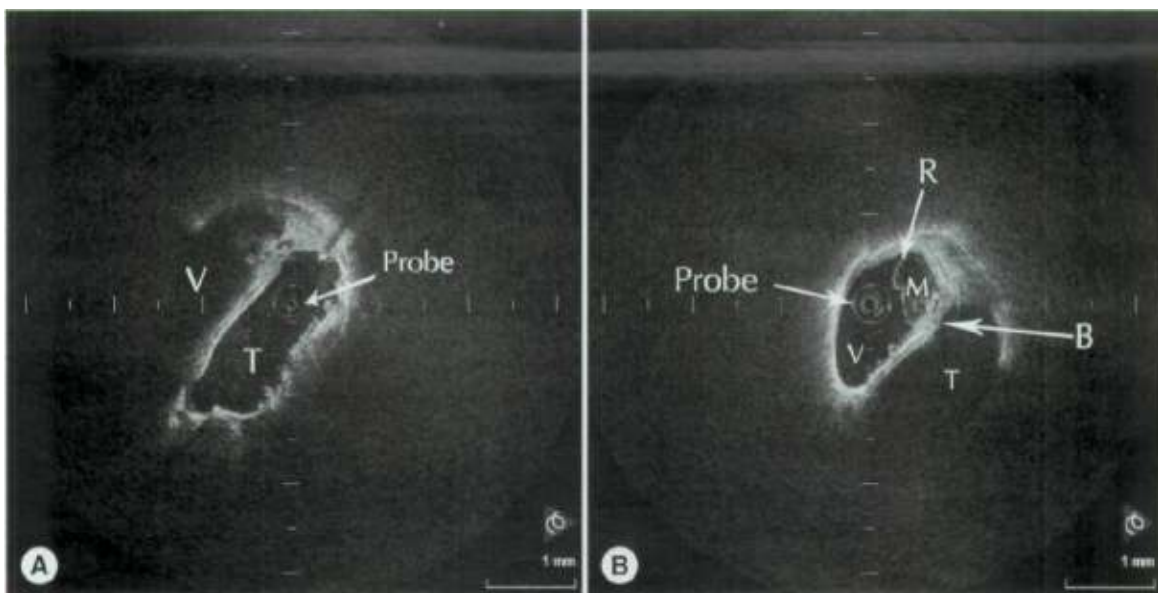
Figure 6 - OCT imaging of inner ear obtained with 0.5 mm probe at 3.1 Hz. [21]. (a) Within scalar tympani (b) Within scala vestibuli.

Several studies has already been done in suing the OCT for imaging of the inner ear and cochlea [20-24]. A relevant study demonstrated catheter-based OCT imaging of the cochlea in live mice and a fresh human cadaver [21]. The system schematic and results are shown in Figures 5 and 6. Accordingly, two OCT catheters were constructed by LightLab Imaging, Inc , and used in this study: one axial-imaging 0.35-mm-diameter catheter and one 0.8-mm-diameter catheter. Each catheter consisted of a thin single-mode optical fiber in the center of the imaging probe extending to its tip. Since catheter-based OCT allows unprecedented real-time viewing of microscopic structures of interest through a small, flexible catheter, it has great potential for a the cochlear implant surgical procedure.

2. Specific Aims

We can summarize the aims of this project under two main categories:

2.1. Clinical Aims

- In order to preserve the natural residual hearing of patients for better restoration results, it is important to avoid intracochlear trauma. Thus, the first goal is to locate the electrode array in Scala-Tympani with no damage to the basilar membrane.
- For better stimulation of the hearing nerve, it is desired to place the electrode array as close to modiolus as possible. The second clinical goal is to achieve this perimodiolar position. This corresponds to a configuration where the electrode seems to hug the inner walls of the cochlea.

2.2. Engineering Aims

- Physiological hand tremor combined with limited visualization and access ports is an obstacle against achieving the aforementioned clinical goals. Our first engineering aim is to eliminate this barrier by integrating the steady-hand robot into the surgical procedure. This requires modification on the robot through appropriate end-effector designs to replace traditional surgery tools without sacrificing from their intuitive feel, and to enhance their functionality if possible.
- The second engineering aim is to guide the electrode towards the optimal location during the insertion phase by implementing virtual fixtures and restricting the motion of the robot end-effector. The virtual fixtures will be defined based on the cochlear model generated out of intra-operative OCT images eventually.

3. System Overview

The developed robotic system uses OCT imaging to generate virtual fixtures and guide the implant during insertion. The interaction between these components is summarized in Figure 7.
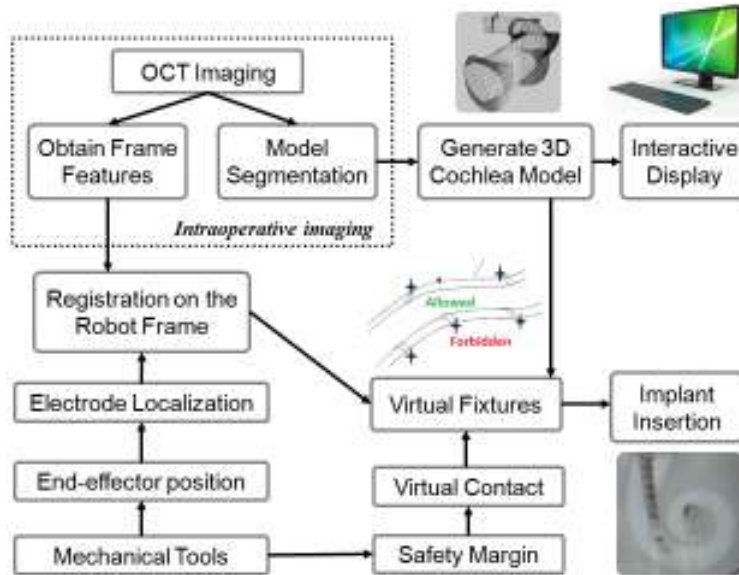
Figure 7 - The workflow and interaction between system components during the surgery.

3.1. Mechanical Tools

In traditional cochlear implant surgery, the Nucleus 24 Contour Advance Electrode (Cochlear Corporation, Inc.) is advanced into the cochlea using tweezers and a hawk tool. For other implants, there exist alternative deployment mechanisms. However, the steps followed during the Advance Off-Stylet remain the same as explained previously on Figure 4. Focusing on the mechanics involved in each of these steps aiming to enhance the functionality of existing manual tools, three different end-effectors for the steady-hand robot were designed, fabricated and tested. Slight differences in the surgical workflow exist depending on the tool selection. A comparison of these concepts is presented in Figure 8.
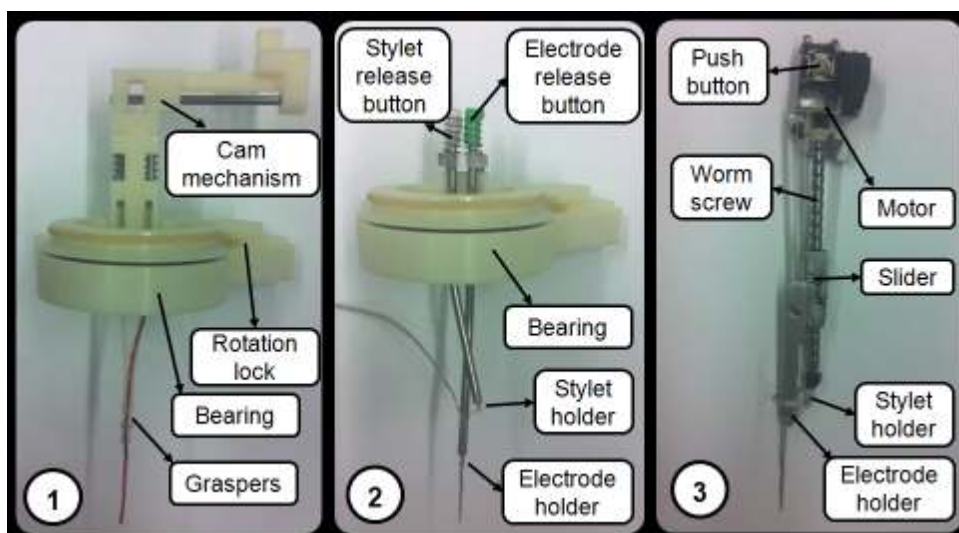
Figure 8 - Concepts for the electrode insertion tool design.

Concept 1: In order to provide axial rotation of the implant, a bearing is attached on the steady-hand robot arm. The hollow center of the bearing allows viewing the operation site through the microscope clearly without significant interference from the tooling. The bearing can be locked by pushing a knob on the handle to fix the axial orientation. The electrode is held from two locations (the same locations as in the traditional manual procedure) via graspers that are attached to the inner ring of the bearing. The graspers are spring-loaded with a tendency to close. They can be opened by rotating a cam on the handle in order to attach and detach the electrode. During the procedure the following steps are followed:

1. The cam is rotated to open graspers. When released, the straight electrode is attached on the spring-loaded tool.

2. The axial rotation of the electrode is corrected and the bearing is locked.

3. Using the steady-hand robot, the implant is inserted until the first basal turn.

4. The graspers are reopened by rotating the cam. The electrode is taken out, and the cam is released to squeeze only the stylet between the graspers.

5. The electrode is held using tweezers and advanced into the cochlear canal until the ribs on the implant reach the cochleostomy site.

Concept 2: In this design, the graspers with the cam mechanism in Concept 1 are replaced by two small forceps mechanisms (one for the electrode, and the other for the stylet) for a better view through the microscope. The forceps are attached to the inner ring of the bearing. They descend into the mastoidectomy site in tubes, which greatly reduce the interference with the microscope view. The forceps are spring loaded and are normally closed. They can be opened by pushing two independent buttons on the bearing. The same workflow as in concept 1 is followed except for the fact that the buttons are used in order to open the graspers rather than turning a cam. The significance of the concept is its compact design and resulting minimized blockage in front of the microscope.

Concept 3: Different than the previous approaches, this concept is a stylus shaped mechanism that can be used to both insert the electrode until the first turn, and deploy it off until reaching the end. In contrast to the previous approaches, no other external tool, such as a tweezer, is needed to complete the procedure. In this design, a worm screw located along the tool provides smooth linear motion to a slider. The slider carries the electrode back and forth, which is used to push the electrode in and out of the cochlear canal. The mechanism can be driven either by hand or by the motor mounted on the top part. In order to advance the electrode manually, the small gear on the top part is turned manually with the thumb while holding the tool with the other fingers. For using the motor, it is enough to push the button on the motor until the slider reaches the end of the track. The stylet of the implant is attached on the tool body to remain

stationary during the deploying-off procedure. For attaching the electrode and the stylet on the slider and the tool body respectively, small springs are used. This is a very simple and compact approach that is powerful enough to rigidly hold the implant without interfering with the microscope view. The main strength of this concept is its compact design. Furthermore, this type of tooling without the motor is very convenient as a disposable insertion tool, which eliminates the concerns for sterilization and associated costs. During the procedure the following steps are followed:

1. The electrode and the stylet are squeezed between the springs on the slider and the tool body respectively.

2. The tool is mounted on the steady-hand robot.

3. The implant is inserted until the first turn using the robot.

4. After reaching the first basal turn, the robot is locked. The small gear on the top part is slowly rotated or the button on the motor is pushed. This causes the slider to move along the tool shaft while deploying the electrode into the cochlea off the stylet.

5. When the slider reaches the limit, the insertion is completed. The electrode is taken out of the spring attachment using tweezers.

6. Holding the electrode fixed with the tweezers, the robot arm is moved away. The stylet remains attached on the tool body, and therefore is completely removed from the implant at the end of this step.

3.2. Virtual Fixtures
In a human-machine system, virtual fixtures can be added as a means of providing guidance that helps a robotic manipulator perform a task by limiting its movement into restricted regions and/or influencing its movement along desired paths. Most previous work on virtual fixtures has used impedance-controlled telemanipulation devices, such as traditional haptic interfaces, where the virtual fixtures are defined as forbidden regions (virtual walls) in the master or slave workspace.

In order to apply virtual fixture for our system we initially used the following method with is more direct and seemed to have a good functionality for our application which incorporates non-redundant structure.

In the Steady-Hand paradigm, the relationship between velocity and motion is derived by considering a virtual contact between the robot tool tip and the environment. In most cases, this contact is modeled by a linear viscous friction law:

$$V = \frac{1}{K} \cdot F$$

Here we call the coefficient 1/k, C or admittance. When using the above equation the robot stiffness in all direction is equal. A virtual fixture generalizes this model to include anisotropic admittances. If delta represents the instantaneous "preferred" directions of motion for the tool tip then the projection matrix is defined as D:

$$D_\delta = \delta(\delta'\delta)^{-1}\delta'$$

Now if we decompose the input force into two components, one in direction of preferred motion and another perpendicular to it, we can rewrite the control law as follows, where a new admittance is introduced which reduces the component of the force input in the non-preferred direction.

$$v = c(f_\delta + c_\tau f_\tau) = c(D_\delta + c_\tau(1 - D_\delta))f = G(c, c_\tau, \delta)f$$

Therefore, the final control law is in the general form of an admittance control with a time-varying matrix G. If we choose $c_\tau = 0$ then it would create hard virtual fixture making it impossible to move in any direction other than the preferred direction. Other cases can be named soft virtual fixtures.

With this concept two types of constraint can be identified as represented in Figure 9. In the Reference Target mode, the robot directs the tool toward a specific point while in the Reference Curve mode the robot constrains the user motion along a 3-D Cartesian path.
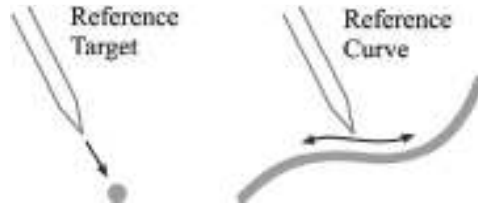
Figure 9 - Two distinct constraint types: Reference Target mode, and Reference Curve mode.

The information from the OCT imaging system is used to identify the reference geometries; however it can be assumed that those references are known. The following function represents the transfer function relating the robot velocity to the human input force:

$$\frac{V_i(s)}{F_i(s)} = \frac{s + (k_p + k_v s)c}{m_i s^2 + (b_i + k_v)s + k_p}$$

However this method has some limitations for implementation since it doesn't consider kinematics of the robot and would be hard to generalize. It assumes that the kinematics is handled elsewhere and therefore only computes the required Cartesian velocities. Of course another processing block can be added at the end of this which can compute the velocities for the robot which is typically required in terms of joint

velocities, which was done for some of the steady hand papers. The limitation of this work is when the robot cannot fulfill the required Cartesian velocities. However as it is mentioned, a solution for this is to use the current Cartesian position of the robot in combination with external sensor which is OCT imaging to compute required Cartesian velocity in a closed loop fashion.

On the other hand, a generalization and combination of both these into one processing block can be done similar to the work done in [28, 29]. In the implementation of this method, in derivation of the joint velocities from Cartesian velocities should be handled very carefully where the configuration is of the robot joints are coupled. It should also be mentioned that the Jacobian of a manipulator is only a first order approximation and therefore finding an iterative solution to the kinematics equations works only for the most non-trivial robot. As a consequence we decided to change our approach to another method, namely constrained control algorithm.

Figure 10 represents virtual fixtures in the context of our application. As it is depicted in Figure 10, once entered the cochlea canal, the surgeon prefers to avoid hitting the walls of the cochlea as well as the basilar turn which is of critical importance.

**Figure 10 -** Implemented virtual fixtures along the cochlear canal.

This method describes a control scheme that provides a link between human understandable task primitives and mathematical robot control. For a given surgical task, these primitives could be combined to address both guidance virtual fixtures and forbidden region virtual fixtures. The method generalizes to systems with either the impedance or admittance type of low-level controller, making controller details transparent to the developer. In order to accommodate uncertainties inherent in surgical tasks, the notion of soft virtual fixtures with absolute bounds. Moreover, the same framework allows us to take into account the constraints of a specific robot. The soft virtual fixtures enable a surgical tool to have some resistance inside boundary regions and no resistance in preferred regions. An extension of constrained optimization control to multiple robot arms is also presented. The constrained optimization problem

identified in work of [28] with both linear and nonlinear constraints is used, and discuss the trade-offs between them.

Typical surgical tasks have a certain degree of uncertainty that arises from factors such as registration errors, variations in anatomy and changes during procedures. Furthermore, we can do another region where the surgeon might deliberately want to place the instrument to account for some uncertainties inherent in surgical procedures. In other words, we would like to have some compliance in the VF, while maintaining a preferred motion. Therefore, three different regions are defined:

a. Allowed region: this region defines the expected outcome.

b. Boundary region: the tool could temporarily be in this region while filling some expected task. (e.g. to compensate for uncertainty in the surgical procedure).

c. Forbidden region: For safety purposes, the tool must never be in this region.

The relationship of these three regions depends on the surgical task. Figure 11 shows each region in this section.
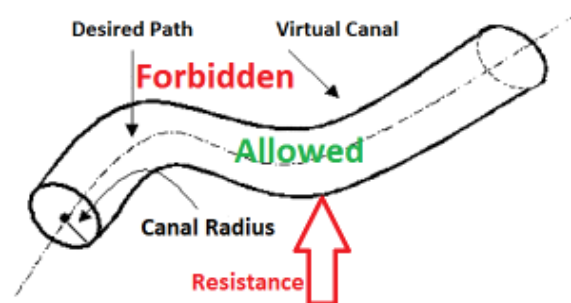

Figure 11 - Three different regions of a typical virtual fixture.

A motion planning algorithm for surgical robots such as our steady hand robot must take into account the uncertainty in tasks and the need to place absolute bounds on motions and also the uncertainty. This algorithm is presented here.

From a perspective of implementing the constraint optimization, the constraints can arise from two sources. The first are required to meet the goals of the geometry of the task and the second to meet certain manipulator requirements.

First, different task frames associated with different parts of the instrument are defined. For each of the task frames, we define actual state variables x and desired state variables xd. The state, x is a function of joint variables q and joint incremental motion. The desired state, is a function of user input and joint variables q.

As mentioned earlier the various basic constraints can be combined to yield a specific behavior from the robot as shown in Figure 12.
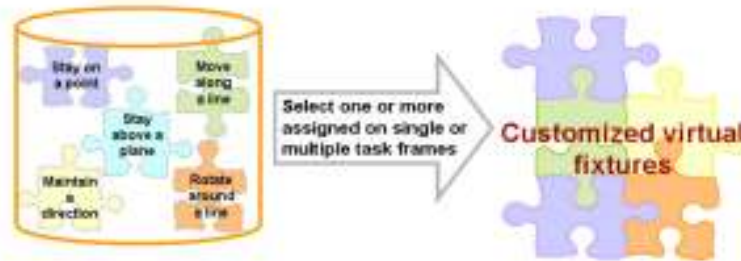

Figure 12 - Implementation of a customized virtual fixture.

In order to achieve our objective to enter the cochlea we are using two task primitives.

1. Stay on a point: Keep the tool position x_t on the reference position x_o. This is represented as $CON_{VF1}(\{i\}, x_0, \varepsilon_1)$

2. Move along a line: Keep the tool position x_t on line L which has the direction $\hat{l}_o$ and passes through point x_o. At the same time, the tool should move along L proportional to the users input. This constraint is written as $CON_{VF3}(\{i\}, [x_0, \hat{l}_0], \varepsilon_3)$

The graphical representation of this phenomenon is shown as follows Figure 13 . The figure on the left shows the restriction to stay on a point while the one on the right constrains the motion on the desired orientation.
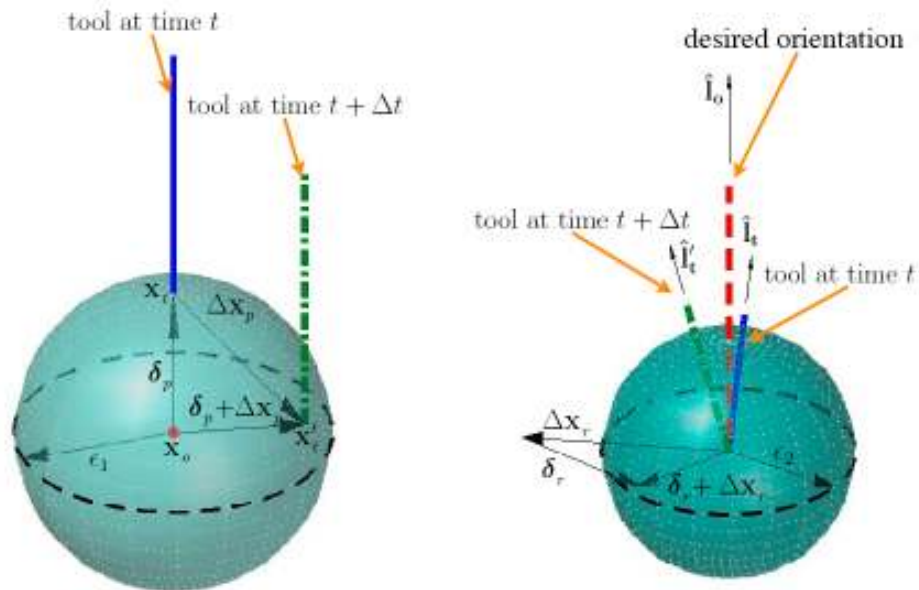
Figure 13 - Constraint for staying on a point (left), and for maintaining a direction (right).

Alternatively one can model a cylinder as it is shown below Figure 14. The polyhedron determined by $A \cdot x < b$ with different numbers of hyperplanes. The inscribed volume, defines the ideal error tolerance region as in Figure 14.
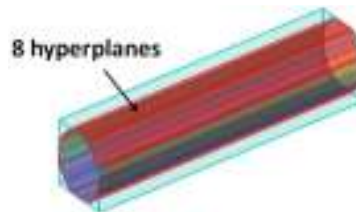

Figure 14 - Cylinder confined by a hyperplane.

In order to solve this problem we need to solve the inequality optimization problem. There are computational trade-offs between linearly constrained and nonlinearly constrained least squares (LS) problems. The algorithms for solving linearly constrained LS problems (such as LS inequality methods, active set methods, etc.) are usually less complex than the algorithms for solving the nonlinearly constrained LS problems (such as reduced-gradient methods, SQP methods, etc.). Solving linearly constrained LS problem can take less computation time. As it is clear this approach generates an optimization problem that leads to non negative least square solving problem.

3.3. OCT Imaging

Optical coherence tomography (OCT) measures the depth-resolved backreflections from a biological tissue with up to sub-micron-level resolution, and can perform imaging at or above the video rate. Optical coherence tomography is analogous to ultrasound imaging but is based on the detection of infrared light waves that are backscattered or reflected from different layers and structures within the tissue. Unlike sound waves, the speed of light is very high, rendering direct electronic measurement of the echo delay of the reflected light (time for the signal to return) impossible. Measurements can be performed using an interferometric correlation technique known as low-coherence interferometry. In an interferometer, a light beam from an optical light source is split into 2 parts, a reference beam and a sample beam. The reference beam is reflected off a mirror at a known distance and returns to the detector. The sample beam reflects off different layers within the tissue, and light returning from the sample and reference arms recombines. If the 2 light beams travel the same distances (optical path length) to within the coherence length of the light, the 2 beams will interfere. If the path lengths are mismatched, there is no interference. Optical coherence tomography measures the intensity of interference of light backscattered or reflected from different points within the tissue by moving the mirror in the reference arm, which changes the distance that light travels in the reference arm. light from a coherent vs a low-coherent light source are shown, illustrating how low-coherence light can be used to localize back-reflection sites and provide the desired

high resolution. 2 or 3-dimensional images are produced by scanning the optical beam across the sample and recording the optical backscattering vs depth at different transverse positions. The resulting image is a 2- or 3-dimensional representation of the optical backscattering of the sample on a micron scale. The logarithm of the backscattering signal is represented as a false color or gray-scale image. A schematic of the complete OCT system is shown in Figure 15.
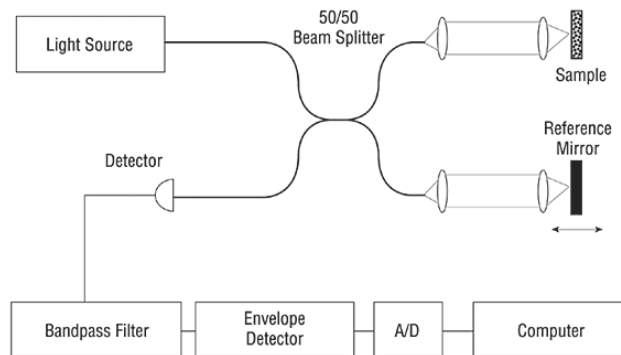
Figure 15 - Schematic of an OCT system.

These unique capabilities have granted OCT numerous applications in medicine and biology [31–34]. Early OCT systems were commonly built on the low coherence interferometry by altering the optical path length in the reference arm of an interferometer and measuring the interferogram in the time domain, which is thus referred to as the time domain OCT (TD-OCT) [35,36].

Our preliminary work with OCT demonstrates the feasibility of OCT for cross-sectional and 3-dimensional imaging of middle ear structures without the need to generate the full 3D model of cochlea. Images correlated well with gross anatomy. The primary focus of this work was to demonstrate the feasibility of OCT imaging of cochlea structure. Additional steps required to examine the ability to fully generate the structure of cochlea in vivo.

For our application different can work, however it should be considered that the important features of the cochlea structure should be found. Using a rotating catheter that is capable of axial motion would be able to generate the full 3 dimensional geometry of the cochlea. Also, by using the objective lens of the microscope as the sample arm one can find the basilar turn of the cochlea which is of critical importance. This would give the virtual fixture the necessary input as to where to stop.

Another important role of the OCT system is for the registration purposes. For any task to be performed appropriately by the robot, the end-effector should be on the same frame of reference with respect to tracking frame. In our case and for the insertion of the implant the framework for generating the virtual fixtures are coming from the OCT system. Therefore, the steady hand robot coordinate system should be registered to frame of which the fixture is built upon. Therefore, prior to manipulation we would obtain robot frame features and make sure that are appropriately registered.

4. Experiments and Results

The developed mechanical tools and implemented virtual fixtures were tested and evaluated by our surgeon, Wade Chien, on an artificial cochlea phantom, which was provided by Cohlear Ltd. In the setup shown in Figure 16, a side viewing camera inside the artificial phantom monitors the cochlear canal only for evaluation purposes. The electrode insertion tool is attached to the robot hand. The steady-hand robot has two foot-pedals. The left pedal is configured to drive the system such that the robot moves according to the direction and magnitude of applied forces. The right pedal is for activating virtual fixtures. The operator drives the system based on the 3D image of the cochleostomy site provided through stereo microscopes. The same image is also reflected on a 3D monitor for convenience. During the tests, the operator first brings the electrode tip to the cochlea entrance by keeping the left pedal of the steady-hand robot pushed. Then, releasing the left and pushing the right pedal, virtual fixtures are activated. When pushed down, the robot inserts the electrode into the cochlea until the first basal turn while keeping the electrode orientation fixed. Before the tip hits the cochlea walls, the robot stops due to implemented virtual fixture. Currently, this is based on a fixed depth from the entrance point, but the goal is to get this information from OCT imaging eventually. After the robot locks, even if the user pushes further down, the electrode will not penetrate. However it can still be removed. The robot prevents only further advancement of the straight electrode, not the removal of it. Then following the appropriate workflow of the utilized tool, insertion is completed. The success is verified based on the electrode location from the side viewing camera.

Figure 16 - Experimental setup.

Our trials have indicated that the implemented virtual fixtures is successful in avoiding collisions with the cochlea walls as well as reducing the effect of physiological hand tremor. Despite the successful results, we observed that the bearing used in tooling concepts 1 and 2 could occasionally block the view of the surgeon during the procedure. Blocking the cochleostomy site with insertion tools and electrode parts is

an already existing problem in traditional surgery. We can solve this problem in our robotic system by designing an adapter with a larger bearing. However, this would also limit the access ports for deploying off the electrode in the final step of the insertion procedure. Thus, it is a matter of optimization to decide on the correct bearing size for this application. Another observation was that starting the procedure with a perfectly straight electrode is much easier compared to a slightly curved one. A brand new electrode has normally a slight curvature that is designed to reduce traumas if the cochlear walls are hit during the procedure. However, this curvature makes it more challenging to bring the electrode tip to the cochleostomy site through the narrow facial recess. Since our robotic system can guarantee that the implant will not be hitting cochlear walls, a stiffer stylet inside the implant can be used to resolve this problem. In this case, the surgeon will be inserting a stiffer but straight array inside the cochlea until reaching the first basal turn, which will be much easier and less-time consuming.

5. Conclusion

In this study, a steady-hand system for cochlear implant insertion was introduced. The designed end-effector has enhanced the functionality of existing manual tool maneuvers. Even though we have not been able to perform expansive statistical evaluation, the preliminary trials have indicated that the implemented virtual fixtures is successful in avoiding collisions with the cochlea walls as well as reducing surgeon's inherent hand tremor. So far, it has been a short study to show the feasibility of the approach for minimally invasive cochlear implant surgery. We are planning to perform substantial number of experiments to show that the preliminary results are statistically significant.

6. Management Summary

6.1. Credits

The project can be segmented into three main parts: mechanical electrode insertion tool design, robot software development, and OCT imaging. The tool development and fabrication was handled by Berk Gonenc under the supervision of Iulian Iordachita and Russell Taylor. Robot control software and virtual fixture implementation was done by Ehsan Azimi with the guidance of Russell Taylor. OCT imaging techniques were developed by Jin Kang and his research group. The generated concepts related to each part were discussed, evaluated and improved together as a team. Based on the input from our surgeons, Wade Chien and John Niparko, the system was modified to fit the needs of implant surgery in the best way.

6.2. Deliverables

The steps related to electrode insertion and virtual fixture implementation were successfully completed within the planned time frame. However, the team has experienced delays in OCT imaging part since many concepts were generated, which are still under evaluation and development.

Delivered:

- Tooling design and fabrication for electrode insertion with the steady-hand robot.
- Procedure workflow for robotically assisted cochlear implantation.
- Robot software with integrated virtual fixtures.
- Implant insertion videos and images.
- Implant insertion demonstration.

To be delivered:

- OCT adapter design and fabrication for the steady-hand robot.
- OCT scanning videos and images.
- OCT system demonstration.

6.3. Future Work

Future studies aim at the following:

- Improvements on the insertion tool design for better ergonomics and wider view through the microscope.
- Design and fabrication of an adapter to hold and rotate the OCT probe with the steady-hand robot for intra-operative imaging.
- Integration of the robotic system (virtual fixtures) with OCT imaging.
- Testing and validation of the complete system on artifical cochlea phantom.
- Experiments on dry temporal bones.
- Experiments on cadaveric bones.

6.4. Lessons Learned

- Microscope field of view and tool compactness is a trade-off, which requires design optimization.
- It is crucial to allocate enough time and get surgeons' feedback during development period.

References

[1] Lenarz T, Stöver T, Buechner A et al (2006) Temporal bone results and hearing preservation with a new straight electrode. Audiol Neurootol 11(Suppl 1):34–41.

[2] Roland P, GstöttnerW,AdunkaO (2005) Method for hearing preservation in cochlear implant surgery. OperativeTech 16(2):93–100.

[3] AdunkaOF, Pillsbury HC,Kiefer J (2006) Combining perimodiolar electrode placement and atraumatic insertion properties in cochlear implantation—fact or fantasy? Acta Otolaryngol 126(5):475–482.

[4] Adunka OF, Radeloff A, Gstoettner WK et al (2007) Scala tympani cochleostomy. II. Topography and histology. Laryngoscope 117(12):2195–2200.

[5] Briggs RJS, Tykocinski M, Stidham K et al (2005) Cochleostomy site: implications for electrode placement and hearingbpreservation. Acta Otolaryngol 125(8):870–876.

[6] Eshraghi AA, Yang NW, Balkany TJ (2003) Comparative study of cochlear damage with three perimodiolar electrode designs. Laryngoscope 113(3):415–419.

[7] Roland PS,WrightCG (2006) Surgical aspects of cochlear implantation: mechanisms of insertional trauma. Adv Otorhinolaryngol 64:11–30.

[8] Stöver T, Issing P, Graurock G et al (2005) Evaluation of the advance off-stylet insertion technique and the cochlear insertion tool in temporal bones. Otol Neurotol 26(6):1161–1170.

[9] Wardrop P, Whinney D, Rebscher SJ et al (2003) A temporal bone study of insertion trauma and intracochlear position of cochlear implant electrodes. I. Comparison of Nucleus banded and Nucleus Contour electrodes. Hear Res 203(1–2):54–67.

[10] Wardrop P,Whinney D, Rebscher SJ et al (2005) A temporal bone study of insertion trauma and intracochlear position of cochlear implant electrodes. II. Comparison of Spiral Clarion and HiFocus II electrodes. Hear Res 203(1–2):68–79.

[11] Hussong A, Rau T, Ortmaier T et al (2010) An automated insertion tool for cochlear implants: another step towards atraumatic cochlear implant surgery. International Journal of Computer Assisted Radiology and Surgery 5:163–171.

[12] United States Patent 7184843: Electrode array with non-uniform electrode spacing.

[13] Cohen LT, Saunders E, Clark GM (2001) Psychophysics of a prototype peri-modiolar cochlear implant electrode array. Hear Res 155(1–2):63–81.

[14] Rau T, Hussong A, Lewinung M et al (2009) Automated insertion of preformed cochlear implant electrodes: evaluation of curling behavior and insertion forces on an artificial cochlear model. International Journal of Computer Assisted Radiology and Surgery 5:173–181.

[15] Hussong A, Rau T, Eilers H et al (2008) Conception and design of an automated insertion tool for cochlear implants. Engineering in Medicine and Biology Society. EMBS 2008. 30th Annual International Conference of the IEEE , pp.5593-5596, 20-25 Aug. 2008.

[16] Schurzig D, Labadie R, Hussong A, Rau T, Webster R (2010) A Force Sensing Automated Insertion Tool for Cochlear Electrode Implantation. IEEE International Conference on Robotics and Automation, May 2010.

[17] Schurzig D, Labadie R, Hussong A, Rau T, Webster R (2012) Design of a Tool Integrating Force Sensing With Automated Insertion in Cochlear Implantation. IEEE/ASME Transactions on Mechatronics, 17(2): 381-389.

[18] Kratchman L, Blachon G, Withrow T et al (2010) Toward Auutomation of Image-Guided Microstereotactic Frames: A bone-Attached Parallel Robot for Percutaneous Cochlear Implantation. Robotics Science and Systems 2010: Workshop on Enabling Technologies.

[19] Kratchman L, Blachon G, Withrow T et al (2011) Design of a Bone-Attached Parallel Robot for Percutaneous Cochlear Implantation. IEEE Transactions on Biomedical Engineering, 58(10):2904-2910.

[20] Thomas S. Rau, Omid Majdani, Andreas Hussong, Thomas Lenarz, Martin Leinung. Determination of the curling behavior of a preformed cochlear implant electrode array", Int J CARS (2011) 6:421–433.

[21] James Lin, MD; Hinrich Staecker, MD, PhD; M. Samir Jafri, PhD "Optical Coherence Tomography Imaging of the Inner Ear: A Feasibility Study With Implications for Cochlear Implantation" Annah of Olülugy, Rhinology & Laryngohgy 117(5):341-346. 2008.

[22] HANS WILHELM PAU, EVA LANKENAU, TINO JUST, DETLEF BEHREND & GEREON HUTTMANN "Optical coherence tomography as an orientation guide in cochlear implant surgery?" Proc. of SPIE Vol. 6842 68421F-1.

[23] Costas Pitris, PhD; Kathleen T. Saunders, BS; James G. Fujimoto, PhD; Mark E. Brezinski, MD, PhD "High-Resolution Imaging of the Middle Ear With Optical Coherence Tomography: A Feasibility Study" ARCH OTOLARYNGOL HEAD NECK SURG/VOL 127, JUNE 2001.

[24] Hrebesh M. Subhash Viviana Davila et al."Volumetric in vivo imaging of intracochlear microstructures in mice by high-speed spectral domain optical coherence tomography" Journal of Biomedical Optics 15_3_, 036024 _May/June 2010.

[25] Daniel Schurzig, Zachariah W. Smith, D. Caleb Rucker, Robert F. Labadie, Robert J. Webster III, A manual insertion mechanism for percutaneous cochlear implantation, Design of Medical Devices Conference (DMD2010), April 13-15 2010, Minneapolis, MN, USA

[26] Ramya Balachandran, Jason E. Mitchell, Jack Noble, Daniel Schurzig, Gregoire Blachon, Theodore R. McRachan, Robert J. Webster, Benoit M. Dawant, J. Michael Fitzpatrick, Robert F. Labadie, Insertion of electrode array using percutaneous cochlear implantation technique: a cadaveric study, Medical Imaging 2011: Visualization, Image-Guided Procedures, and Modeling, February 13 2011, Lake Buena Vista, FL, USA

[27] Daniel Schurzig, Robert F. Labadie, Andreas Hussong, Thomas S, Rau, Robert J. Webster, A Force Sensing Automated Insertion Tool for Cochlear Electrode Implantation, IEEE International Conference on Robotics and Automation, May 2010

[28] A. Kapoor, M. Li, and R. H. Taylor, "Constrained control for surgical assistant robots," in IEEE International Conference on Robotics and Automation, 2006,pp. 231_236.

[29] M. Li, A. Kapoor, and R. H. Taylor, "A constrained optimization approach to virtual fixtures, in IEEE/RSJ International Conference on Intelligent Robots and Systems, 2005, pp. 1408-1413.

[30] P. Marayong and A. M. Okamura, "Speed-Accuracy Characteristics of Human-Machine Cooperative Manipulation Using Virtual Fixtures with Variable Admittance," Human Factors, Vol. 46, No. 3, pp. 518-532, 2004.

[31] M. E. Brezinski, Optical Coherence Tomography: Principle and Practice (Academic, Burlington, 2006).

[32] M. E. Brezinski and J. G. Fujimoto, "Optical coherence tomography: high-resolution imaging in nontransparent tissue," IEEE J. Sel. Top. Quantum Electron. 5(4), 1185–1192 (1999).

[33] M. E. Brezinski, G. J. Tearney, B. E. Bouma, J. A. Izatt, M. R. Hee, E. A. Swanson, J. F. Southern, and J. G. Fujimoto, "Optical coherence tomography for optical biopsy. Properties and demonstration of vascular pathology," Circulation 93(6), 1206–1213 (1996).

[34] G. J. Tearney, M. E. Brezinski, B. E. Bouma, S. A. Boppart, C. Pitris, J. F. Southern, and J. G. Fujimoto, "In vivo endoscopic optical biopsy with optical coherence tomography," Science 276(5321), 2037–2039 (1997).

[35] D. Huang, E. A. Swanson, C. P. Lin, J. S. Schuman, W. G. Stinson, W. Chang, M. R. Hee, T. Flotte, K. Gregory, C. A. Puliafito, and J. G. Fujimoto, "Optical coherence tomography," Science 254(5035), 1178–1181 (1991).

[36] G. J. Tearney, B. E. Bouma, and J. G. Fujimoto, "High-speed phase- and group-delay scanning with a gratingbased phase control delay line," Opt. Lett. 22(23), 1811–1813 (1997).